Method for Nonstationary Jammer Suppression in Noise Radar Systems

Slobodan Djukanović, Miloš Daković, Thayananthan Thayaparan, LJubiša Stanković

Abstract— **Noise radars represent a rapidly growing research topic owing to numerous advantages over the conventional radars. This paper proposes a method for strong nonstationary jammer suppression in noise radar systems. The corrupted received signal is divided into non-overlapping segments so that the instantaneous frequency (IF) of the jammer can be approximated by a parabola within each segment. To that end, an adaptive recursive procedure is proposed. The procedure uses the polynomial-phase transform to estimate the parabola coefficients. The jammer suppression is done for each segment separately. The simulations, performed for various types of FM interferences, prove the effectiveness of the proposed method even for highly nonstationary jammers with non-polynomial phase.**

I. Introduction

Noise radars exhibit numerous advantages over the conventional ones due to truly random transmitting signal. The advantages include unambiguous range estimation, high immunity to noise, interference suppression, low probability of intercept, high electromagnetic compatibility, ideal thumbtack ambiguity function.

In the past decade, a significant research has been devoted to the development and implementation of random noise radar [1]–[6]. Recent research has investigated the potential use of noise radar for the ultrawide-band SAR/ISAR imaging, Doppler and polarimetric measurements, collision warning, detection of buried objects and targets obscured by foliage. Wide bandwidth provides a high range resolution, while an extended pulse length reduces the peak power. A non-periodic waveform suppresses the range ambiguity while reducing both the probability of intercept and the interference influence.

IET Signal Processing, Vol. 4, No. 3, June 2010.

The real time digital range/Doppler processing puts strong requirements on computing speed, but, on the other hand, provides increased flexibility in performance. The binary or low-bit ADC significantly improves the signal-processing rate and reduces the costs [5]. The average peak-to-sidelobe ratio (PSR) is for the single reflector case similar for both the binary and high-resolution ADC. For the multiple reflectors case, the binary ADC is outperformed by the high-resolution one for approximately 4dB. A comprehensive analysis of the performance of phase- and frequency-modulated noise radar is presented in [6], including a study on the main factors that influence the range sidelobes, analysis of phase and frequency modulation by noise, investigation of the range sidelobe suppression and performance, investigation of biphase modulation by random noise, analysis of clutter influence on the sidelobe level.

Even though random noise radar is a rapidly growing research topic, very little attention has been devoted to the jamming problem. A strong jammer can significantly reduce the PSR of the received signal and therefore deteriorate the performance of receiver [7]. Numerous available methods for nonstationary jammer suppression in direct sequence spread spectrum (DSSS) systems can be used with noise radars, since DSSS signals are also wide-band signals. In [16], the author introduces the nonstationary jammer excision for signals characterized by their instantaneous frequencies. Time-frequency (TF) based methods are among most attractive. Let us mention non-parametric methods based on the short-time Fourier transform (STFT) [17] and the local polynomial Fourier transform [18], and parametric method based on the generalized Wigner-Hough transform [19].

In this paper, we propose a simple method for filtering the noise radar return corrupted by a high-power broadband jammer. The jammer covers both the frequency and time ranges of the operating noise radar. The received signal is divided into non-overlapping segments so that, for each segment separately, the instantaneous frequency (IF) of the jammer can be sufficiently well approximated by a parabola. The parabola coefficients are obtained by using the discrete polynomial-phase transform (DPT) [11]–[13]. The DPT is chosen over other parameter estimation methods (see [8]–[10], [14], and corresponding references) for its simplicity. Knowing the jammer's IF trajectory [8], we can dechirp the received signal in order to move the jammer to the zero frequency (DC), and filter it by excising only its DC component. The proposed method is evaluated for various types of FM interferences. An approximation to the PSR after the jammer suppression is derived and numerically verified.

The theoretical background, including the basics of random noise radar and the DPT, is given in Section II. The proposed jammer suppression method is presented in Section III. Numerical examples are given in Section IV.

II. Theoretical background

A. Noise radar basics

In noise radar systems, a random noise signal is transmitted, reflected from a target, and received with a delay $T = \frac{2r}{c}$, where r and c respectively denote the distance from the target and the speed of light. The received signal is correlated with a replica of the transmitted noise delayed by T_r. The correlation peak, arising for $T = T_r$, indicates the distance from the target. On the other hand, Doppler filters, at the correlator output, give the velocity of the target [2], [3].

Let us consider a radar transmitting a complex stationary Gaussian random noise $x(t)$ with the variance σ_x^2. We will assume that a single point scatterer is located at the range r_0 along the radar line-of-sight (LOS). The received signal $y\,(t)$ can be modeled as

$$y(t) = A_\sigma x(t - T_0) + \varepsilon(t), \tag{1}$$

where A_σ denotes the target reflectivity, $T_0 = \frac{2r_0}{c}$ is the round-trip delay and $\varepsilon(t)$ is an undesired part of the received signal which will be modeled as additive white Gaussian noise (AWGN) with the variance σ_ε^2. Moreover, $x\,(t)$ and $\varepsilon\,(t)$ are uncorrelated with each other. Without loss of generality, we will adopt $A_\sigma = 1$. The correlation between the received and delayed transmitted signal can be written as

$$C(\tau) = \int_0^{T_{int}} y(t)x^*(t-\tau)dt, \tag{2}$$

where T_{int} is the integration time. Due to finite T_{int}, $C(\tau)$ is also a random variable characterized by mean

$$\begin{aligned} E\left[C(\tau)\right] &= \int_0^{T_{int}} E[y\left(t\right)x^*\left(t-\tau\right)]dt \\ &= \int_0^{T_{int}} E\left[x\left(t-T_0\right)x^*\left(t-\tau\right)\right]dt \\ &+ \int_0^{T_{int}} E\left[\varepsilon\left(t\right)x^*\left(t-\tau\right)\right]dt \\ &= \int_0^{T_{int}} R_{xx}\left(\tau - T_0\right)dt \\ &= T_{int}R_{xx}(\tau - T_0), \end{aligned} \tag{3}$$

where $R_{xx}(\tau)$ represents the autocorrelation function of $x(t)$. Having in mind that $|R_{xx}(\tau)| \leq R_{xx}(0)$ [20], the delay T_0 can be estimated as

$$T_0 = \max_\tau \left|E\left[C(\tau)\right]\right|. \tag{4}$$

The randomly fluctuating correlation, however, can be analyzed in a simpler way by describing the correlation integral as follows [5], [6]:

$$\begin{aligned} C_k &= \sum_{n=0}^{N-1} y\left(n\right)x^*\left(n-k\right) \\ &= \sum_{n=0}^{N-1} \left[x\left(n-m\right) + \varepsilon\left(n\right)\right]x^*\left(n-k\right), \end{aligned} \tag{5}$$

where $x(n)$ is a sequence of random complex numbers with $E[x(n)] = 0$ and $E[x(n)x^*(l)] = \sigma_x^2\delta(n-l)$, integers m and k respectively correspond to T_0 and τ, and N represents the number of independent samples corresponding to the integration time T_{int}. Clearly, a strong correlation peak occurs at $k = m$.

In order to evaluate the performance of the correlation receiver, the PSR is introduced as follows [5]:

$$\mathrm{PSR} = \frac{E^2[C_{k=m}]}{\mathrm{Var}[C_{k\neq m}]}. \tag{6}$$

Substituting (5) into (6) yields [5], [6]

$$\mathrm{PSR} = \frac{N^2\sigma_x^4}{N\sigma_x^4 + N\sigma_x^2\sigma_\varepsilon^2} = \frac{N}{1+\mathrm{SNR}^{-1}}, \tag{7}$$

where $\mathrm{SNR} = \sigma_x^2/\sigma_\varepsilon^2$ represents the signal-to-noise ratio (SNR), where the term noise in this definition corresponds to the AWGN.

B. The discrete polynomial-phase transform

Consider a constant amplitude signal $x(n)$ with the Qth order polynomial phase $\varphi(n)$,

$$x(n) = Ae^{j\sum_{m=0}^{Q} a_m(n\Delta)^m},\ 0 \le n \le N-1, \tag{8}$$

where N is the number of samples, a_m are real coefficients and Δ represents the sampling interval. Next we define operators [12], [13]

$$\begin{aligned}
&\mathrm{DP}_1[x(n),\tau] = x(n)\\
&\mathrm{DP}_2[x(n),\tau] = x(n)x^*(n-\tau)\\
&\vdots\\
&\mathrm{DP}_M[x(n),\tau] = \mathrm{DP}_2[\mathrm{DP}_{M-1}[x(n),\tau],\tau],
\end{aligned} \tag{9}$$

where M is the operator order and τ is the delay parameter.

For $M = Q$, $\mathrm{DP}_M[x(n),\tau]$ outputs a single tone with frequency

$$\omega_0 = M!(\tau\Delta)^{M-1}a_M \tag{10}$$

implying that a_M can be estimated simply by estimating ω_0. On the other hand, if $M > Q$, $\mathrm{DP}_M[x(n),\tau]$ outputs a constant.

The DPT of order M (DPT_M) is defined as the discrete-time Fourier transform of $\mathrm{DP}_M[x(n),\tau]$ [12], [13], i.e.

$$\mathrm{DPT}_M[x(t),\omega,\tau] = \sum_{n=(M-1)\tau}^{N-1} \mathrm{DP}_M[x(n),\tau]e^{-j\omega n\Delta}. \tag{11}$$

Therefore, for $M = Q$, DPT_M has a single spectral line at ω_0 given by (10), whereas for $M > Q$, DPT_M has a spectral line at the zero frequency.

The DPT-based estimator is computationally efficient and robust to slowly time-varying amplitude and non-polynomial (but continuous) phase, and it provides estimation accuracy very close to the CR bound (see [12, eq. (42)-(47)]). On the other hand, for this estimator to operate properly, the required SNR should satisfy (see [12, eq. (58)])

$$N\ \mathrm{SNR} \ge 25\binom{2M-2}{M-1} \tag{12}$$

and it increases rapidly with the phase polynomial order.

In addition, in order to properly estimate a_M, ω_0 must not exceed the Nyquist frequency, and therefore

$$|a_M| \le \frac{\pi}{M!\tau^{M-1}\Delta^M} \tag{13}$$

is required [12, eq. (15)]. By reducing Δ we can extend the range of values of a_M that can be unambiguously estimated.

Finally, we will choose the value of τ according to

$$\tau = \begin{cases} \frac{N}{M} & \text{for } M = 2 \text{ and } M = 3\\ \frac{N}{M+2} & \text{for } M \ge 4, \end{cases} \tag{14}$$

which is shown to minimize the mean-square error of the a_M estimation [12].

For example, the coefficients of a third-order polynomial phase can be estimated as follows:

***Step* 1.** Set $\tau = \frac{N}{3}$ and estimate a_3 as

$$\widehat{a}_3 = \frac{\arg\max_{\omega}\{|\mathrm{DPT}_3[x(n),\omega,\tau]|\}}{3!(\tau\Delta)^2}. \tag{15}$$

***Step* 2.** Set $\tau = \frac{N}{2}$ and estimate a_2 as

$$\widehat{a}_2 = \frac{\arg\max\limits_{\omega} \{|\mathrm{DPT}_2 [x_3(n), \omega, \tau]|\}}{2!\tau\Delta}, \quad (16)$$

where $x_3(n) = x(n)\, e^{-j\widehat{a}_3(n\Delta)^3}$.

***Step* 3.** Estimate a_1 as

$$\widehat{a}_1 = \arg\max_{\omega} \{|\mathrm{DPT}_1 [x_{23}(n), \omega, \tau]|\}, \quad (17)$$

where $x_{23}(n) = x(n)\, e^{-j\left[\widehat{a}_2(n\Delta)^2 + \widehat{a}_3(n\Delta)^3\right]}$.

The estimates $\widehat{a}_3$, $\widehat{a}_2$ and $\widehat{a}_1$ may be effectively obtained by using an iterative procedure proposed in [14].

III. A DPT based interference suppression

A. Influence of jammer

Let us assume that the received sequence $y(n)$, apart from the sequences $x(n)$ and $\varepsilon(n)$, contains a jammer sequence $J(n)$, that is

$$y(n) = x(n) + \varepsilon(n) + J(n), \quad 0 \le n \le N-1. \quad (18)$$

All the three sequences are uncorrelated with each other. In addition, the constant-amplitude model for $J(n)$ is adopted,

$$J(n) = Ae^{j\varphi(n)}, \quad (19)$$

where $\varphi(n)$ represents the phase of $J(n)$. The signal-to-jammer ratio (SJR) is defined as $\mathrm{SJR} = \sigma_x^2/A^2$.

Substituting (18) and (19) into (5) gives

$$\begin{aligned} E[C_{k=m}] &= N\sigma_x^2 \\ \mathrm{Var}[C_{k\neq m}] &= N\sigma_x^4 + N\sigma_x^2\sigma_\varepsilon^2 + NA^2\sigma_x^2 \end{aligned}$$

and the corresponding PSR value, denoted as PSR_J, equals

$$\mathrm{PSR}_J = \frac{N}{1 + \mathrm{SNR}^{-1} + \mathrm{SJR}^{-1}}. \quad (20)$$

This PSR can be dramatically reduced for $\mathrm{SJR} \ll 1$, implying that $y(n)$ has to be preprocessed before the correlation is performed.

A simple and computationally efficient method for high-power jammer suppression in noise radar systems is introduced in the following section.

B. Proposed method

According to the Weierstrass's approximation theorem, we can approximate the jammer's phase $\varphi(n)$ by a polynomial assuming that the original phase function $\varphi(t)$ is continuous within an observed time interval. We propose to divide the received signal into nonoverlapping segments so that, for each segment separately, $\varphi(n)$ can be approximated by a third-order polynomial, or equivalently, the IF of the jammer can be approximated by a parabola. Next step is to dechirp segments in order to dislocate the jammer power to the zero frequency. The jammer is suppressed in the frequency domain by excising only the DC component of the dechirped segment.

The jammer suppression can be performed in an adaptive manner by using the following recursive procedure.

***Step* 1.** Estimate the phase coefficients of the jammer by using (15)–(17).

***Step* 2.** Form $\theta(n) = \widehat{a}_1(n\Delta) + \widehat{a}_2(n\Delta)^2 + \widehat{a}_3(n\Delta)^3$ and dechirp $y(n)$ according to $y_\theta(n) = y(n)\, e^{-j\theta(n)}$.

***Step* 3.** Calculate $Y_\theta(p) = \mathrm{DFT}[y_\theta(n)]$. If the jammer spectrum for $p \neq 0$ can be neglected, suppress the jammer by excising the DC component $Y_\theta(0)$. After excising $Y_\theta(0)$ and chirping the signal back, we obtain the filtered signal $y'(n)$ as

$$y'(n) = \left(\frac{1}{N}\sum_{p=1}^{N-1} Y_\theta(p)\, e^{j\frac{2\pi}{N}np}\right) e^{j\theta(n)} \quad (21)$$

or alternatively

$$y'(n) = y(n) - \frac{1}{N}Y_\theta(0)\, e^{j\theta(n)}. \quad (22)$$

However, if the jammer spectrum for $p \neq 0$ cannot be neglected, perform the steps 1–3 for both the left half and the right half of the observed signal $y(n)$.

The decision whether the jammer power contained within $Y_\theta(p)$, $p \neq 0$, can be neglected is made by observing the vicinity of $Y_\theta(0)$. Ideally, after dechirping, the whole jammer is contained within $Y_\theta(0)$ and the filtering is optimal. In addition, $|Y_\theta(p)|$ for $p \neq 0$

represents a Rayleigh variable with scale parameter $b_0 = \sigma_{x\varepsilon}/\sqrt{2}$, where $\sigma_{x\varepsilon} = \sqrt{\sigma_x^2 + \sigma_\varepsilon^2}$. We will denote such a variable as Y_0. The mean and variance of Y_0 are defined as [20]

$$\begin{array}{l} \mu_{Y_0} = \sqrt{\frac{\pi}{2}} b_0 \\ \sigma_{Y_0}^2 = \left(2 - \frac{\pi}{2}\right) b_0^2. \end{array} \tag{23}$$

In reality, however, the dechirped jammer is spread over other DFT coefficients. The low-frequency components of $Y_\theta(p)$ contain more jammer than the high-frequency ones (see Fig. 2). We will therefore assume that the jammer contained within $Y_\theta(p)$ for $p \neq 0$ can be neglected if

$$|Y_\theta(p)| < \mu_{Y_0} + 4\sigma_{Y_0}, \quad p = 1, 2, ..., K, \tag{24}$$

where μ_{Y_0} and σ_{Y_0} are defined by (23) and K is the number of considered samples. Note that $P\left(Y_0 \geq \mu_{Y_0} + 4\sigma_{Y_0}\right) = 5.5121 \times 10^{-4}$.

One way to estimate the standard deviation $\sigma_{x\varepsilon}$, and in turn b_0, is from a TF representation of the received signal. For this purpose we can use the simplest TF representation, the STFT. In the TF plane, $J(n)$ occupies a narrow frequency band compared to both the radar return and the AWGN that are uniformly spread over all frequencies [7]. $\sigma_{x\varepsilon}$ can be estimated from the variance of the STFT bins that belong to the TF areas where the jammer contribution can be neglected.

Finally, by observing the steps of the proposed method, as well as (15)–(17) and the frequency estimation procedure presented in [14], we can conclude that the overall computational complexity is $\mathrm{O}(N \log_2 N)$, where $\mathrm{O}(\cdot)$ represents the big O notation. On the other hand, the TF-based jammer suppression methods have the complexity of $\mathrm{O}\left(N^2 \log_2 N\right)$ [16]–[18].

C. PSR after the jammer suppression

Let L represent the number of signal segments obtained in the filtering procedure. The segment lengths are N_1, N_2, ..., N_L. The correlation (5) after the filtering, denoted as C'_k, satisfies

$$\begin{aligned} C'_k &= \sum_{l=1}^{L} \sum_{n=0}^{N_l-1} y'\left(n + \sum_{i=1}^{l-1} N_i - m\right) \\ &\quad \times x^*\left(n + \sum_{i=1}^{l-1} N_i - k\right) \\ &= \sum_{l=1}^{L} \sum_{n=0}^{N_l-1} y'_{lm}(n)\, x^*_{lk}(n) = \sum_{l=1}^{L} C'_{kl}, \end{aligned} \tag{25}$$

where the definitions of $y'_{lm}(n)$, $x^*_{lk}(n)$ and C'_{kl} are clear from (25). Consider C'_{kl}. First, by using (21), we get

$$\begin{aligned} y'_{lm}(n) &= \left(\frac{1}{N_l} \sum_{p=1}^{N_l-1} Y^\theta_{lm}(p)\, e^{j\frac{2\pi}{N_l}np}\right) e^{j\theta(n)} \\ &= \frac{1}{N_l} \sum_{p=1}^{N_l-1} \sum_{q=0}^{N_l-1} y_{lm}(q)\, e^{j\frac{2\pi}{N_l}p(n-q)} e^{j(\theta(n)-\theta(q))}. \end{aligned} \tag{26}$$

Inserting (26) into the C'_{kl} expression yields

$$\begin{aligned} C'_{kl} &= \frac{1}{N_l} \sum_{n,q} \sum_{p} y_{lm}(q)\, x^*_{lk}(n) \\ &\quad \times e^{j\frac{2\pi}{N_1}p(n-q)} e^{j(\theta(n)-\theta(q))} \\ &= \frac{1}{N_l} \sum_{n,q} \sum_{p} (x_{lm}(q) + \varepsilon_{lm}(q))\, x^*_{lk}(n) \\ &\quad \times e^{j\frac{2\pi}{N_l}p(n-q)} e^{j(\theta(n)-\theta(q))}, \end{aligned} \tag{27}$$

where n and q run from 0 to $N_l - 1$, while p runs from 1 to $N_l - 1$. We will assume that, after the filtering, the residual jammer can be neglected. The jammer sequence $J_{lm}(q)$ was therefore omitted in (27). This assumption will be numerically justified in the Simulations section.

The expectation of C'_{kl} for $k = m$ equals

$$\begin{aligned} E[C'_{kl}] &= \frac{\sigma_x^2}{N_l} \sum_{n,q} \sum_{p} \delta(n-q) \\ &\quad \times e^{j\frac{2\pi}{N_l}p(n-q)} e^{j(\theta(n)-\theta(q))} \\ &= (N_l - 1)\, \sigma_x^2. \end{aligned}$$

On the other hand, $E[C'_{kl}]$ for $k \neq m$ equals

$$\begin{aligned} E[C'_{kl}] &= \frac{1}{N_l} \sum_{n,q} \sum_{p} E[x_{lm}(q) x^*_{lk}(n)] \\ &\quad \times e^{j\frac{2\pi}{N_l}p(n-q)} e^{j(\theta(n)-\theta(q))} \end{aligned}$$

which, by using

$$E\left[x_{lm}\left(q\right)x_{lk}^{*}\left(n\right)\right]=$$
$$E\left[x\left(q+\sum_{i=1}^{l-1}N_i-m\right)x^{*}\left(n+\sum_{i=1}^{l-1}N_i-k\right)\right]$$
$$=\sigma_x^2\delta\left(q-m-n+k\right),$$

becomes

$$E\left[C'_{kl}\right]=\frac{\sigma_x^2}{N_l}\sum_{n,q}\sum_{p}\delta\left(q-m-n+k\right)$$
$$\times e^{j\frac{2\pi}{N_l}p(n-q)}e^{j(\theta(n)-\theta(q))}$$
$$=\frac{\sigma_x^2}{N_l}\sum_{n}\sum_{p}e^{-j\frac{2\pi}{N_l}p(m-k)}e^{j(\theta(n)-\theta(n+m-k))}$$
$$=-\frac{\sigma_x^2}{N_l}\sum_{n}e^{j(\theta(n)-\theta(n+m-k))}.$$

In the previous relation, we used the identity

$$\sum_{p=1}^{N_l-1}e^{-j\frac{2\pi}{N_l}p(m-k)}=\begin{cases}-1 & k\neq m\\ N_l-1 & \text{otherwise.}\end{cases}$$

Since $\sum_{n=0}^{N_l-1}e^{j(\theta(n)-\theta(n+m-k))}$ represents the DC component of $e^{j(\theta(n)-\theta(n+m-k))}$, it can be neglected for $\theta\left(n\right)\neq const.$ Therefore, for $k\neq m$, we have

$$E\left[C'_{kl}\right]\approx 0. \tag{28}$$

As for the variance $\mathrm{Var}[C'_{kl}]$, we have

$$\mathrm{Var}[C'_{kl}]=$$
$$\frac{1}{N_l^2}\sum_{n_1,n_2,q_1,q_2}\sum_{p_1,p_2}E[(x_{lm}(q_1)+\varepsilon_{lm}(q_1))$$
$$\times(x_{lm}^{*}(q_2)+\varepsilon_{lm}^{*}(q_2))x_{lk}^{*}(n_1)x_{lk}(n_2)]$$
$$\times e^{j\frac{2\pi}{N_l}(p_1(n_1-q_1)-p_2(n_2-q_2))}$$
$$\times e^{j(\theta(n_1)-\theta(q_1)-\theta(n_2)+\theta(q_2))}$$
$$=\frac{1}{N_l^2}\sum_{n_1,n_2,q_1,q_2}\sum_{p_1,p_2}E[x_{lm}(q_1)x_{lm}^{*}(q_2)$$
$$\times x_{lk}^{*}(n_1)x_{lk}(n_2)]e^{j\frac{2\pi}{N_l}(p_1(n_1-q_1)-p_2(n_2-q_2))}$$
$$\times e^{j(\theta(n_1)-\theta(q_1)-\theta(n_2)+\theta(q_2))}$$
$$+\frac{1}{N_l^2}\sum_{n_1,n_2,q_1,q_2}\sum_{p_1,p_2}E[\varepsilon_{lm}(q_1)\varepsilon_{lm}^{*}(q_2)$$
$$\times x_{lk}^{*}(n_1)x_{lk}(n_2)]e^{j\frac{2\pi}{N_l}(p_1(n_1-q_1)-p_2(n_2-q_2))}$$
$$\times e^{j(\theta(n_1)-\theta(q_1)-\theta(n_2)+\theta(q_2))}. \tag{29}$$

Since both $x_{lm}\left(n\right)$ and $\varepsilon_{lm}\left(n\right)$ are zero mean Gaussian variables, the following relations hold [20]:

$$E[x_{lm}(q_1)x_{lm}^{*}(q_2)x_{lk}^{*}(n_1)x_{lk}(n_2)]=$$
$$\sigma_x^4\delta(q_1-q_2)\,\delta(n_1-n_2)$$
$$+\sigma_x^4\delta\left(q_1-m-n_1+k\right)\delta\left(q_2-m-n_2+k\right)$$

$$E[\varepsilon_{lm}(q_1)\varepsilon_{lm}^{*}(q_2)x_{lk}^{*}(n_1)x_{lk}(n_2)]=$$
$$\sigma_x^2\sigma_\varepsilon^2\delta(q_1-q_2)\delta(n_1-n_2)$$

and, by inserting these relations into (29), we obtain

$$\mathrm{Var}\left[C'_{kl}\right]=\left(N_l-1\right)\sigma_x^2\left(\sigma_x^2+\sigma_\varepsilon^2\right). \tag{30}$$

Now (25) implies that

$$E\left[C'_{k=m}\right]=\sum_{l=1}^{L}\left(N_l-1\right)\sigma_x^2=\left(N-L\right)\sigma_x^2$$
$$\mathrm{Var}\left[C'_{k\neq m}\right]=\sum_{l=1}^{L}\left(N_l-1\right)\sigma_x^2\left(\sigma_x^2+\sigma_\varepsilon^2\right)$$
$$=\left(N-L\right)\sigma_x^2\left(\sigma_x^2+\sigma_\varepsilon^2\right).$$

Finally, the PSR after the filtering of the received signal, denoted as PSR′, satisfies

$$\mathrm{PSR}'=\frac{E^2\left[C'_{k=m}\right]}{\mathrm{Var}\left[C'_{k\neq m}\right]}=\frac{N-L}{1+\mathrm{SNR}^{-1}}. \tag{31}$$

For $L\ll N$, PSR′ approximately equals the PSR given by (7).

D. Multicomponent jammer case

The DPT is a nonlinear transform and for multicomponent signals it will, apart from the DPTs of individual components (auto-terms), produce undesired cross-terms. Depending on the amplitudes of signal components, these cross-terms can completely cover auto-terms.

For example, assume that the jammer $J(n)$ comprises two cubic-phase components with amplitudes A_1 and A_2, where $A_1>A_2$. The operator $\mathrm{DP}_3\left[J\left(n\right),\tau\right]$ outputs two complex sinusoids with amplitudes A_1^4 and A_2^4 (auto-terms), as well as eight cubic-phase and two quadratic-phase cross-terms. The amplitude of the strongest cross-term is $2A_1^3A_2$; therefore

the proper estimation of stronger component requires $A_1 > 2A_2$.

Assuming that the number of jammer components, N_J, is known and the component amplitudes allow the estimation of auto-terms, we can suppress it starting from the strongest component. The procedure is as follows [13]:

***Step* 1.** Set $k = 1$.

***Step* 2.** If $k = N_J$ go to step 4. Otherwise, estimate the phase coefficients of the strongest component using the DPT, which results in $\theta(n)$.

***Step* 3.** Suppress the jammer component by using (22). Set $k = k + 1$ and go to step 2.

***Step* 4.** Estimate $\theta(n)$ of the last component and dechirp the received signal. If the jammer spectrum at K lowest frequencies (bins) of the dechirped signal, excluding the DC component, can be neglected, suppress the jammer. Otherwise, perform the steps 1–3 for the left half and the right half of the observed signal.

This algorithm is very similar to the filtering procedure proposed in [13], with the difference that herein we, instead of noise, suppress the signal whose phase is estimated. The use of the algorithm is, however, restricted to simple cases when the amplitudes of components considerably differ.

In the Simulations section, the proposed algorithm is evaluated on the received signal containing a two-component jammer.

IV. Simulations

Consider a noise radar operating at the carrier frequency $f_0 = 10$GHz with the bandwidth $B = 204.8$MHz and the pulse duration of $T_r = 40\mu s$. The transmitted signal is reflected from a single point scatterer target located at the distance $r_0 = 1.5$km. We assume that the sampling rate, at baseband, equals the Nyquist rate $\Delta = 1/B$; therefore one pulse contains $N = 8192$ samples. The received signal is corrupted by the AWGN so that SNR $= \frac{1}{20}$ (or -13dB).

The received signal contains a jammer defined by (19). Table I presents phase function $\varphi(n)$ of five considered jammer types, each of them satisfying SJR $= \frac{1}{1000}$ (or -30dB). The first three types are polynomial phase jammers, i.e., constant frequency, linear FM and quadratic FM jammer, whereas the fourth and the fifth type correspond to exponential FM and sinusoidal FM jammer, respectively. Evolution of the IF versus time for all the jammer types is depicted in Fig. 1.

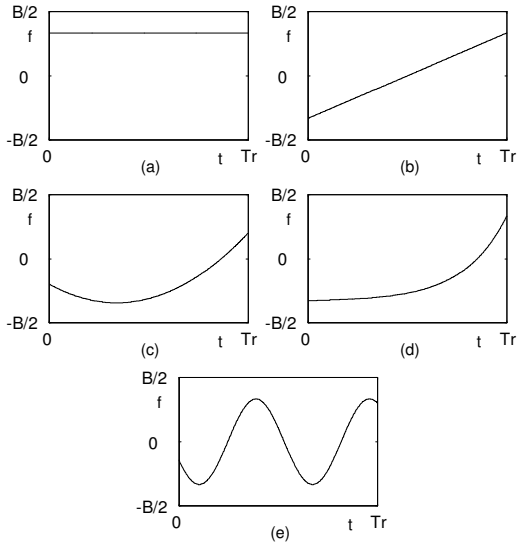

Fig. 1. The instantaneous frequency of jammers defined in Table I. (a) Stationary jammer. (b) Linear FM jammer. (c) Quadratic FM jammer. (d) Exponential FM jammer. (e) Sinusoidal FM jammer.

The analytical value of the PSR, according to (7), for the adopted values of the SNR and SJR, is PSR = 390.1. Numerical PSR values, obtained over 1000 filtering realizations, without and with the jammer suppression are presented in Table II. The rightmost column of Table II gives the average number of segments, $\overline{L}$, obtained in the filtering procedure over all the realizations. We used $K = 3$ samples in the decision procedure (24).

The numerical PSR′ values clearly justify that the influence of the residual jammer can be neglected in our analysis. The flatness of the spectrum around the DC component of the dechirped signal $y_\theta(n) = y(n)\, e^{-j\theta(n)}$ indicates how well does a parabola, determined by the estimates $\widehat{a}_1$, $\widehat{a}_2$ and $\widehat{a}_3$, approximate the jammer's IF function within the considered

TABLE I
PHASE FUNCTIONS OF CONSIDERED JAMMERS

	Jammer's phase $\varphi(n)$
Type 1	$2\pi\frac{B}{3}(n\Delta)$
Type 2	$2\pi(-\frac{B}{3}(n\Delta)+\frac{B^2}{3N}(n\Delta)^2)$
Type 3	$2\pi(-\frac{B}{5}(n\Delta)-\frac{17B^2}{40N}(n\Delta)^2+\frac{5B^3}{12N^2}(n\Delta)^3)$
Type 4	$2\pi(\frac{4N}{B\ln(2B/3)}(\frac{2B}{3})^{\frac{3}{4}}e^{\frac{B\ln(2B/3)}{4N}(n\Delta)}-\frac{B}{3}(n\Delta))$
Type 5	$2\pi\frac{2N}{21\pi}\cos(\frac{7\pi B}{2N}(n\Delta)+\frac{\pi}{7})$

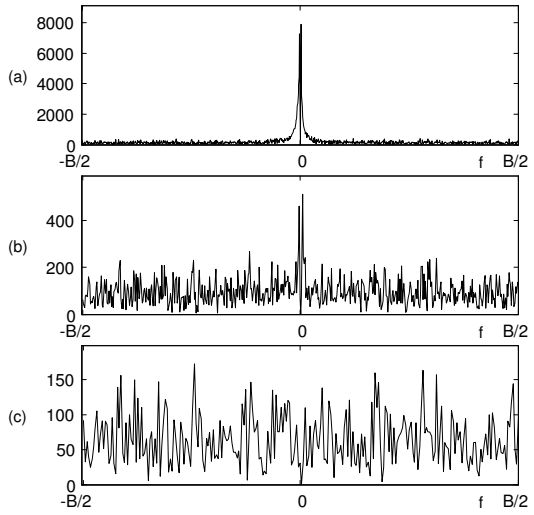

Fig. 2. The spectrum of the dechirped parts of the received signal corrupted by the fifth jammer type. The parts correspond to first (a) $N/8$ samples; (b) $N/16$ samples; (c) $N/32$ samples.

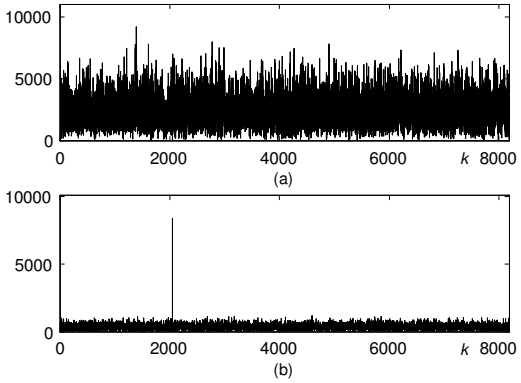

Fig. 3. The absolute value of correlation, $|C_k|$, for a single point scatterer: (a) before the jammer suppression and (b) after the jammer suppression.

segment. In accordance with Section III-B, if the jammer's IF is well approximated within the whole signal, i.e., N samples, we do the filtering (22); otherwise, we split the signal into two halves and separately perform the IF estimation on both halves, first left then right. By reducing the observed segment length we also reduce the IF variation we deal with. If the IF estimation obtained for the left half (first $N/2$ samples) is sufficiently well, we filter the left half; otherwise, we split the left half into its left half and right half and so forth. Once we filter the current left half, we repeat the procedure for the corresponding right half. In this way, the whole signal is segmented in an adaptive manner so that the length of each segment equals $\frac{N}{2^k}$, where $k = 0, 1, 2...$ Furthermore, within each segment, the IF variation can be approximated by a parabola, which is the criterion for stopping further segment splitting.

Consider, for example, the fifth type of jammer. We first operate on N samples, then on first $N/2$ samples (left half), then on first $N/4$ samples (left half of the left half), then $N/8$ samples. The spectra of the dechirped parts of the received signal, where the parts correspond to its first $N/8$, $N/16$ and $N/32$ samples, are shown in Fig. 2(a), (b) and (c), respectively. The DC component is excised. The first $N/32$ samples will not be further split since the jammer is well concentrated at the DC component (i.e., the rest of the spectrum is sufficiently flat), which is not the case for $N/8$ and $N/16$.

The absolute value of correlation (25), for one realization of the received signal corrupted by the fifth jammer type, is depicted in Fig. 3. More precisely, Fig 3(a) depicts the value

TABLE II
PSR VALUES AND AVERAGE NUMBER OF SEGMENTS $\overline{L}$

	Supp. off	Supp. on	$\overline{L}$
Type 1	8.11	383.76	1.003
Type 2	7.99	399.53	1.010
Type 3	8.14	392.19	1.001
Type 4	8.07	382.78	11.854
Type 5	7.89	395.30	27.492
Type 2 + Type 3	6.13	380.74	1.009

TABLE III
POSITION OF TARGETS AND CORRESPONDING SJRS

	Position	SJR
Target 1	1.1km	-27.31dB
Target 2	1.3km	-28.76dB
Target 3	1.5km	-30dB
Target 4	1.7km	-31.09dB
Target 5	1.9km	-32.05dB
Target 6	2.1km	-32.92dB
Target 7	2.3km	-33.71dB

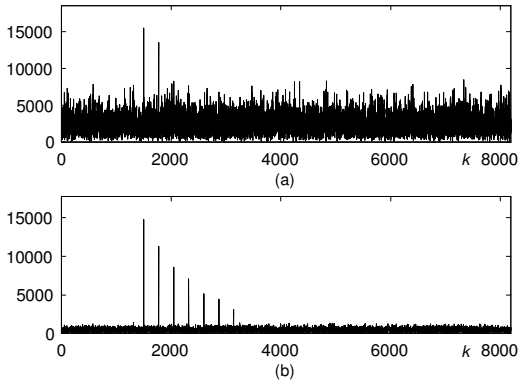

Fig. 4. The absolute value of correlation, $|C_k|$, for multiple targets: (a) before the jammer suppression and (b) after the jammer suppression.

TABLE IV
PSR VALUES FOR BINARY AND LOW-BIT ADCS

	Supp. off	Supp. on
Binary	1.02	1.14
Low-bit 2 bits	3.37	39.66
Low-bit 3 bits	8.51	169.96
Low-bit 4 bits	7.75	299.91
Low-bit 8 bits	7.81	373.16

of $|C_k|$ when no jammer suppression is performed, whereas Fig. 3(b) depicts the value of $|C'_k|$ after implementation of the proposed method.

The last row of Table II corresponds to the multicomponent jammer case. In specific, we considered a two-component jammer whose components correspond to the Type 2 and Type 3 jammers from Table I. The components are characterized by SJR $= -25$dB and -30dB, respectively.

We will briefly illustrate the case of multiple targets. In specific, we will assume that, in addition to the above considered target, six more targets exist, thus making a system of seven targets. All targets are modeled as single point scatterers. The target positions are given in Table III. The received signal is corrupted by the Type 5 jammer. The SJRs for radar returns from all the targets are also given in Table III. Fig. 4 shows the value of $|C_k|$ before and after the jammer suppression. Without the jammer suppression, we are still able to detect two targets that are closest to the receiver since they have higher SJR than other targets, which are completely covered by correlation sidelobes. However, after applying the proposed filtering method, all the seven targets are successfully detected. The decreasing trend of the $|C'_k|$ peak values in Fig. 4(b) is due to the fact the received signal's power decreases with the fourth power of the distance.

In the previous examples, the high-resolution ADC is considered. Let us, in the end, evaluate the performance of the binary and low-bit ADCs in a strong jamming environment. Low-bit ADCs with 2, 3, 4 and 8 bits are considered. The received signal is

corrupted by the Type 3 jammer with SJR = −30dB. The PSR values are given in Table IV. Only the binary ADC does not work properly with a strong jammer. The low-bit ADC with 8 bits performs nearly as the high-resolution ADC.

V. Conclusion

A method for nonstationary jammer suppression in noise radar systems is proposed. The corrupted received signal is divided into non-overlapping and non-equal length segments. Within each segment, the IF of the jammer is approximated by a parabola, which is, in turn, used for jammer suppression. The proposed method is fast and efficient and it performs well for both polynomial and non-polynomial jammer's phase. It can be also extended to the multicomponent jammers case given that the amplitudes of components considerably differ.

In the future work, we will focus on improving the proposed method so it can suppress multicomponent jammers without amplitude-related restrictions.

References

[1] Bell, D.C., and Narayanan, R.M.: 'Theoretical aspects of radar imaging using stochastic waveforms', *IEEE Trans. Signal Process.*, 2001, 2, (49), pp. 394-400.

[2] Narayanan, R.M., Xu, Y., Hoffmeyer, P.D., and Curtis, J.O.: "Design, performance, and applications of a coherent ultrawideband random noise radar," *Optical Engineering*, 1998, 6, (37), pp. 1855-1869.

[3] Narayanan, R.M., and Dawood, M.: 'Doppler estimation using a coherent ultra wide-band random noise radar', *IEEE Trans. Antennas Propagat.*, 2000, 6, (48), pp. 868-878.

[4] Theron, I.P., Walton, E.K., Gunawan, S., and Cai, L.: 'Ultrawide-band noise radar in the VHF/UHF band', *IEEE Trans. Antennas Propagat.*, 1999, 6, (47), pp. 1080-1084.

[5] Axelsson, S.R.J.: 'Noise radar for range/Doppler processing and digital beamforming using low-bit ADC', *IEEE Trans. Geosci. Remote Sens.*, 2003, 12, (41), pp. 2703-2720.

[6] Axelsson, S.R.J.: 'Noise radar using random phase and frequency modulation', *IEEE Trans. Geosci. Remote Sens.*, 2004, 11, (42), pp. 2370-2384.

[7] Daković, M., Thayaparan, T., Djukanović, S., Stanković, Lj.: 'Time-frequency-based nonstationary interference suppression for noise radar systems', *IET Radar, Sonar & Navigation*, 2008, 4, (2), pp. 306-314.

[8] Boashash, B.: 'Estimating and interpreting the instantaneous frequency of a signal - Part 2: Algorithms and applications', *Proc. IEEE*, 1992, 4, (80), pp. 540-568.

[9] O'Shea, P.: 'A fast algorithm for estimating the parameters of a quadratic FM signal', *IEEE Trans. Signal Process.*, 2004, 2, (52), pp. 385-393.

[10] O'Shea, P.: 'A new technique for estimating instantaneous frequency rate', *IEEE Signal Processing Lett.*, 2002, 8, (9), pp. 251-252.

[11] Peleg, S., and Porat, B.: 'Estimation and classification of polynomial phase signals', *IEEE Trans. Inf. Theory*, 1991, 3, (37), pp. 422-430.

[12] Peleg, S., and Friedlander, B.: 'The discrete polynomial-phase transform', *IEEE Trans. Signal Process.*, 1995, 8, (43), pp. 1901-1914.

[13] Peleg, S., and Friedlander, B.: 'Multicomponent signal analysis using the polynomial-phase transform', *IEEE Trans. Aerosp. Electron. Syst.*, 1996, 1, (32), pp. 378-387.

[14] Aboutanios, E., and Mulgrew, B.: 'Iterative frequency estimation by interpolation on Fourier coefficients', *IEEE Trans. Signal Process.*, 2005, 4, (53), pp. 1237-1242.

[15] Sun, W., and Amin, M.G.: 'A self-coherence anti-jamming GPS receiver', *IEEE Trans. Signal Process.*, 2005, 10, (53), pp. 3910-3915.

[16] Amin, M.G.: 'Interference mitigation in spread spectrum communication systems using time-frequency distributions', *IEEE Trans. Signal Process.*, 1997, 1, (45), pp. 90-101.

[17] Ouyang, X., and Amin, M.G.: 'Short-time Fourier transform receiver for nonstationary interference excision in direct sequence spread spectrum communications', *IEEE Trans. Signal Process.*, 2001, 4, (49), pp. 851-863.

[18] Stanković, Lj., and Djukanović, S.: 'Order adaptive local polynomial FT based interference rejection in spread spectrum communication systems', *IEEE Trans. Instrumentat. Meas.*, 2005, 12, (54), pp. 2156-2162.

[19] Barbarossa, S., and Scaglione, A.: 'Adaptive time-varying cancellation of wideband interferences in spread-spectrum communications based on time-frequency distributions', *IEEE Trans. Signal Process.,* 1999, 4, (47), pp. 957-965.

[20] Papoulis, A.: *Probability, random variables, and stochastic processes*, (McGraw-Hill, New York, 1991, 3rd edition).